

Smithsonian

Contributions to Astrophysics

VOLUME 2, NUMBER 11

THE STATISTICS OF METEORS IN THE EARTH'S ATMOSPHERE

by Gerald S. Hawkins and Richard B. Southworth



SMITHSONIAN INSTITUTION

Washington, D. C.

1958

Publications of the Astrophysical Observatory

This series, *Smithsonian Contributions to Astrophysics*, was inaugurated in 1956 to provide a proper communication for the results of research conducted at the Astrophysical Observatory of the Smithsonian Institution. Its purpose is the "increase and diffusion of knowledge" in the field of astrophysics, with particular emphasis on problems of the sun, the earth, and the solar system. Its pages are open to a limited number of papers by other investigators with whom we have common interests.

Another series is *Annals of the Astrophysical Observatory*. It was started in 1900 by the Observatory's first director, Samuel P. Langley, and has been published about every 10 years since that date. These quarto volumes, some of which are still available, record the history of the Observatory's researches and activities.

Many technical papers and volumes emanating from the Astrophysical Observatory have appeared in the *Smithsonian Miscellaneous Collections*. Among these are *Smithsonian Physical Tables*, *Smithsonian Meteorological Tables*, and *World Weather Records*.

Additional information concerning these publications may be secured from the Editorial and Publications Division, Smithsonian Institution, Washington, D. C.

FRED L. WHIPPLE, Director,
Astrophysical Observatory,
Cambridge, Mass. *Smithsonian Institution.*

The Statistics of Meteors in the Earth's Atmosphere

By Gerald S. Hawkins¹ and Richard B. Southworth²

The heights of occurrence and the velocities of meteors in the atmosphere are of considerable interest to workers both in pure research and in technical problems of the upper atmosphere. From such studies we not only learn facts relating to astronomy and the physics of the upper atmosphere, but we also establish values of some of the environmental parameters above the stratosphere. Numerous data have been collected at Harvard College Observatory from photographic programs using conventional cameras and the Baker Super-Schmidt cameras, and the data have been analyzed by Whipple (1943, 1954), Whipple and Jacchia (1957a), and others. Previous work emphasized the measurement of the deceleration of the meteoroid, both to obtain accurate orbits and to estimate the density of the upper atmosphere. Since this emphasis might possibly have biased the sample of reduced meteors in favor of the longer, brighter trails, we decided to analyze a random sample of about 300 trails by an accurate reduction method.

Before presenting the results of the analysis, it is convenient to summarize contemporary meteor theory to provide a background for interpreting the meteor statistics.

Basic theory of the meteoric processes

Basic meteor theory as it exists today results from the work of a number of people, including particularly Marris, Sparrow, Hoppe, Öpik, and Whipple (see Whipple, 1943).

Let us suppose that a meteoroid of mass m , irregular dimensions, and internal density ρ_m , enters the upper atmosphere with velocity v . Because of the high velocity, the kinetic energy of the incoming body exceeds the

internal energies necessary to pulverize, melt, or vaporize the material.

Air particles are trapped momentarily on or near the surface of the meteoroid, imparting to it the energy of collision and decreasing its forward momentum. The air particles are given a forward velocity while the meteoroid suffers a deceleration, dv/dt , so that by the principle of conservation of momentum we may write

$$m \frac{dv}{dt} = -\Gamma S \rho v^2, \quad (1)$$

where ρ is the density of the atmosphere, Γ is the drag coefficient and S is the effective cross-sectional area of the meteoroid. It is convenient to eliminate one variable from this equation by expressing the cross section as a function of the mass m . If, for example, the meteoroid were a sphere of density ρ_m , the cross sectional area S could be written,

$$S = \left(\frac{9\pi}{16}\right)^{\frac{1}{4}} \rho_m^{-\frac{1}{4}} m^{\frac{3}{4}}. \quad (2)$$

In general, the meteoroid will be an irregularly shaped object, and we must replace the $(9\pi/16)^{\frac{1}{4}}$ by a general dimensionless shape factor A which for bodies of simple shape, such as cones, ellipsoids, and short cylinders, is of the order of unity. With this transformation we can establish the first fundamental equation in the meteor theory, the drag equation:

$$\frac{dv}{dt} = -\Gamma A \rho_m^{-\frac{1}{4}} m^{-\frac{1}{4}} \rho v^2. \quad (3)$$

From the principle of the conservation of energy we may equate the energy imparted by

¹ Boston University and Harvard College Observatory.

² Harvard College Observatory.

the colliding particles to the energy required for ablation (vaporization, melting, or fragmentation) of the meteoroid, since the kinetic energy lost by deceleration of the meteoroid is negligible. Thus

$$\xi \frac{dm}{dt} = -\frac{1}{2} \Lambda A \rho_m m^{\frac{3}{2}} \rho v^3, \quad (4)$$

where ξ is the energy required to ablate one gram of the meteoroid and Λ is the efficiency of the energy exchange. The second fundamental equation, the mass equation, is obtained by dividing equation (4) by equation (3), which gives

$$\frac{1}{m} \frac{dm}{dt} = \frac{\Lambda}{2\Gamma\xi} v \frac{dv}{dt}. \quad (5)$$

The material ablated from the surface of the meteoroid collides with the particles of the atmosphere with the forward velocity v , and hence each meteor atom has a kinetic energy of from 100 to 1000 electron volts. This energy is sufficient to ionize and excite the air particles with consequent emission of light. If the fraction of the kinetic energy converted into light is τ , then the luminous intensity I may be expressed as

$$I = -\frac{1}{2} \left(\frac{dm}{dt} \right) v^2 \tau. \quad (6)$$

Similarly, if β is the probability that an evaporated meteor atom will produce an ion pair, then the number q , of ion pairs per cm of track, is given by the expression,

$$q = -\frac{dm}{dt} \frac{1}{v} \frac{\beta}{\mu}, \quad (7)$$

where μ is the mean mass of an evaporated atom. Thus we have four basic equations in the meteor theory, equations (3), (5), (6), and (7), with mass, velocity, and time as three variables. There are six unknown quantities, Γ , Λ , ρ_m , ξ , τ , and β , which are approximately constant. Two of the variables, v and t , can be evaluated observationally, but m at present is unknown. From the four equations we can evaluate three additional quantities, and this represents the crucial problem facing meteor theory at present. We choose to evaluate the following groups of constants: $\tau/\rho_m^{\frac{3}{2}}(\Gamma A)^3$, $\Lambda/2\Gamma\xi$, τ/β . To evaluate

$\tau/\rho_m^{\frac{3}{2}}(\Gamma A)^3$, we use the fact that the mass at time t is given by integrating equation (6) from t to t_e (the end of the meteor); and on substituting this value of m in the drag equation, we find that

$$\frac{\tau}{\rho_m^{\frac{3}{2}}} (\Gamma A)^3 = -2 \left(\frac{1}{\rho v^3} \frac{dv}{dt} \right)^3 \int_t^{t_e} \frac{I}{v^3} dt. \quad (8)$$

In practice, v is found to be approximately constant and may be brought outside the integral sign. The intensity I is found from the estimated visual magnitude M_v from the expression given by Öpik (1937):

$$M_v = 24.6 - 2.5 \log_{10} I. \quad (9)$$

The quantity $\sigma = \Lambda/2\Gamma\xi$ is found in a similar way by inserting m and dm/dt in the mass equation:

$$\frac{1}{\sigma} = \frac{2\Gamma\xi}{\Lambda} = -\frac{v}{I} \frac{dv}{dt} \int_t^{t_e} I dt. \quad (10)$$

To express τ/β in terms of measured quantities, we eliminate the mass between equations (6) and (7) obtaining the relation, $I = qv^3 \mu \tau / 2\beta$. Substitution for I in equation (9) yields the radar-magnitude relationship

$$M_v = 80.35 - 2.5 (3 \log_{10} v + \log_{10} \frac{\tau}{\beta} + \log_{10} q) \text{ (c.g.s. units)} \quad (11)$$

from which τ/β can be found.

For computational work and for theoretical reasons it is useful to develop subsidiary equations from the basic theory. For example, we may eliminate dm/dt between equations (6) and (4), to obtain the intensity equation, which expresses the intensity of light as a function of air density and meteor velocity:

$$I = \frac{\Lambda A m^{\frac{3}{2}}}{4\xi \rho_m^{\frac{3}{2}}} \tau \rho v^5. \quad (12)$$

By logarithmic differentiation we may then determine the air density, ρ_{max} , at which the meteoroid attains its maximum luminosity:

$$\rho_{max} = \frac{\rho_m^{\frac{3}{2}} m_{max}^{\frac{3}{2}} \cos Z_R}{5H\Gamma A \left\{ \frac{\Lambda v^2}{15\Gamma\xi} + 1 \right\}}. \quad (13)$$

It will be noticed that the differential $d\rho/dt$ has been evaluated by assuming an isothermal atmosphere with a scale height H , and that the meteor enters the atmosphere at an angle Z_R to the vertical with negligible deceleration. Since $\Delta v^2/15\Gamma\zeta \gg 1$, equation (13) simplifies to the form,

$$\rho_{max} = \frac{3\rho_m^{3/2} m_{max}^{1/2} \zeta \cos Z_R}{\Delta H A v^2}. \quad (14)$$

We may express the mass of the meteor in terms of its height h in the atmosphere and its mass m_∞ outside the atmosphere by integrating equation (4):

$$m^{1/2} = m_\infty^{1/2} + \frac{\Delta A v^2}{6\zeta\rho_m^{3/2} \cos Z_R} \int_{+\infty}^h \rho dh. \quad (15)$$

Evaluating the integral by assuming an isothermal atmosphere, and substituting for ρ_{max} from equation (14), we may deduce the simple relationship

$$m_{max} = \frac{8}{27} m_\infty. \quad (16)$$

The intensity of a meteor is given a simple formulation if an isothermal atmosphere is again assumed and ρ_{max} is substituted in the intensity equation. By neglecting deceleration it can be shown that

$$\frac{I}{I_{max}} = \frac{q}{q_{max}} - \frac{9}{4} \frac{\rho}{\rho_{max}} \left[1 - \frac{\rho}{3\rho_{max}} \right]^2. \quad (17)$$

Thus within the limits of the approximation, the normalized light curves of all the meteors are identical when plotted as a function of height, and are independent of velocity, angle of approach, and any physical characteristics of the meteoroid. The integrations involved in equations (12) to (17), of course, are not valid if the meteoroid explodes or produces flares of light along its path, which are frequent occurrences in the brighter photographic meteors, or where the atmospheric scale height varies with height.

It must be emphasized that the theory just outlined has been developed on the assumption of a single meteor body. Recent research has indicated that meteors are composed of collections of fine fragments (Jacchia, 1955), and the theory may require revision to account for the behavior of such conglomerates. In the extreme case of fragmentation, however, it can

probably be stated that the above theory applies to each individual fragment, and can be extended to cover the case of a fragmenting meteor if account can be taken of all the individual particles.

Selection and method of reduction

The meteors were selected from the Baker Super-Schmidt photographs taken from stations at Doña Ana and Soledad, New Mexico, from February 1952 to July 1954. These photographs form a homogeneous and fairly continuous record of the night sky, the major interruptions being caused by periods of moonlight. The principle of the classical decimation process was used to ensure the selection of a random sample, every tenth meteor being chosen for analysis. It was found that some 13 percent of the selected meteors had previously been reduced by Jacchia (unpublished), by the method of Whipple and Jacchia (1957b); these results, marked by an asterisk, have been incorporated in tables 1 and 2. Occasionally the "tenth" meteor selected by our system could not be used, because one of the trails had less than five measurable dashes, or because both images of the meteor cut the edge of the film. In such cases, amounting to less than 10 percent of the total sample, another meteor, immediately preceding (or immediately following) the original choice, was used as a substitute. A group of 13 meteors photographed between December 11 and December 13, 1952, was omitted from the analysis as they were thought to be members of the Geminid stream which is adequately represented in the sample. Careful inspection later showed that 10 of these meteors were actually Geminids. The omission of the three non-Geminids, of course, will bias the sample to some small extent.

The original sample comprised 292 meteors. During the analysis, one of these was rejected when we found that the two photographic images were not of the same meteor. Subsequently, we reduced an additional 69 meteors, selected from the same films that recorded those first chosen. This process, of course, interferes with the original method of selection, but does not appreciably alter the essential randomness of the method. The total sample, therefore, contained 361 meteors.

The "short trail" method of reduction was used as described by Hawkins (1957).

The data

The fundamental data for each meteor are summarized in table 1, which gives sporadic meteors, and table 2, giving meteors in the recognized streams. Meteors are listed in order of their time of appearance and the date is given in days and fractions of days in universal time. To obtain the time of appearance in local mean time at the Doña Ana Station, 0.29667 must be subtracted from the date given in the table. It should be remembered that 10 meteors have been omitted from table 2 (see page 351), with characteristics similar to the Geminid meteors already listed in that table; and that 3 other meteors have been omitted during the same period.

The various quantities appearing in the tables have the following probable errors:

Date, universal time: ± 0.00001 (± 1 second of time). Height above sea level in km, h : ± 0.5 km (uncertainty ± 1 shutter segment).

Apparent radiant, epoch 1950: ± 7 minutes of arc. Cosine of the angle between the observed apparent radiant and the zenith of Doña Ana Station, $\cos Z_{AR}$: correct to 3 decimals.

Velocity corrected for the deceleration in the atmosphere in km/sec, V_∞ : the probable error is given individually. This error includes the effects of uncertainties in determining the radiant position and measuring the segments of the trail. It also takes account of the average shutter flutter to be expected and includes a term for the uncertainty introduced by adopting a standard value of $\sigma (= 10^{-11})$. No probable errors are given for the meteors previously analyzed by Jacchia, because these were long trails, of superior quality, for which the error in V_∞ was less than 0.1 km/sec.

Maximum absolute photographic magnitude, M_{pm} : ± 0.3 . To obtain the absolute visual magnitude, an index varying between 1.8 for bright meteors and 1.0 for faint ones must be added to the photographic magnitude (Jacchia, unpublished).

ΔM , the rise of the meteor magnitude above plate limit: ± 0.2 .

Discussion

Velocity distribution. Figure 1 is a histogram showing the velocity distribution of all shower and sporadic meteors in our sample. The distribution is bimodal and shows a peak at a velocity of 22 km/sec and another at 67 km/sec. The minimum between 45 and 55 km/sec repre-

sents meteors in either of two types of relatively unlikely orbits. One type consists of retrograde orbits with small inclinations to the ecliptic and semimajor axes between 0.7 and 2.5. Orbits of this shape are rare in the photographic records and it is difficult to visualize a process by which meteors could be injected into these orbits, or move into them under the action of perturbations. The second type meets the earth's orbit nearly perpendicularly, and has a

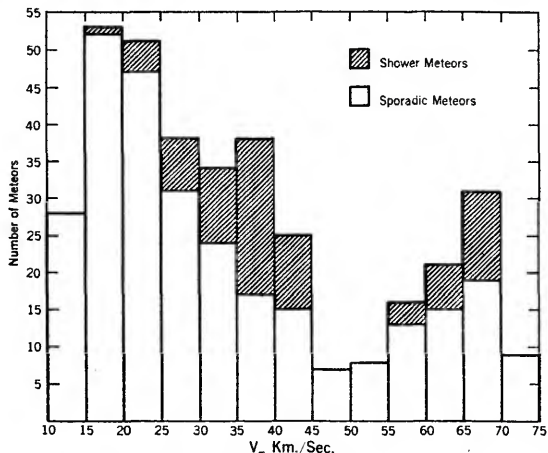


FIGURE 1.—Distribution of corrected velocities, V_∞ , for 285 sporadic and 74 shower meteors.

semimajor axis between 2 and ∞ . Meteors of this second group, which also have radiants near the ecliptic, are almost linear oscillators and the probability is high of their colliding with the sun or the outer corona.

Shower meteors have been indicated separately in the diagram; they clearly tend to be concentrated in two ranges, between 25 and 45 km/sec and between 55 and 70 km/sec. These effects are caused in part by the Geminid stream with a mean velocity of 36.2 km/sec, and by the Orionid stream with a velocity of 67.7 km/sec. There is a noticeable dearth of showers with a velocity less than 25 km/sec. The velocity distribution determined photographically here differs to a small extent from the distribution that may be deduced from the published results of brighter meteors (Whipple, 1954). The present analysis has been carried out to a fainter limiting magnitude, namely +4.5 visual, and there has been no attempt to select brighter meteors or those of longer

duration. The distribution shown here is therefore more representative of photographic meteors than previous results.

Dependence of height on velocity. From equation (14) it can be seen that the simplified theory predicts

$$\log_e \rho_{max} = \log_e \frac{K_1}{v^2}, \quad (18)$$

where

$$K_1 = \frac{3\rho_m^{3/4} \zeta m_{max}^{1/4} \cos Z_R}{\Lambda H A}. \quad (19)$$

Now for an isothermal atmosphere,

$$\rho_{max} = \rho_0 e^{-\frac{h_{max}}{H}}, \quad (20)$$

and when we substitute for ρ_{max} in equation (18),

$$h_{max} = H \log_e \rho_0 - H \log_e \frac{K_1}{v^2}. \quad (21)$$

The mean height of beginning, maximum light, and end have been evaluated for various velocities and are shown in figure 2. From the atmosphere established by the Rocket Panel (1952) we may deduce that $H=6.38$

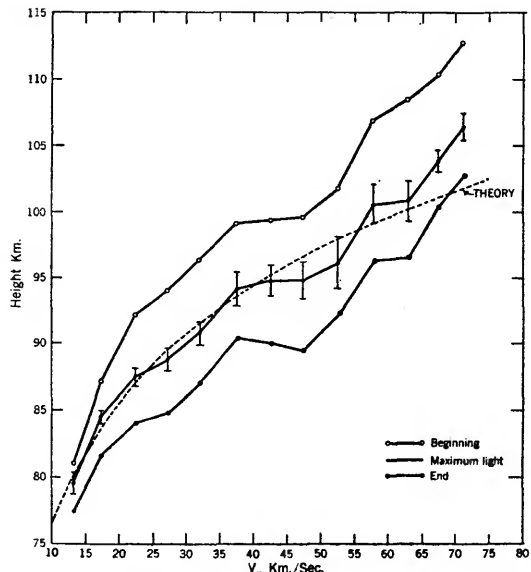


FIGURE 2.—Mean heights of beginning, maximum light, and end for sporadic meteors of various velocities. Broken line indicates theoretical height-curve.

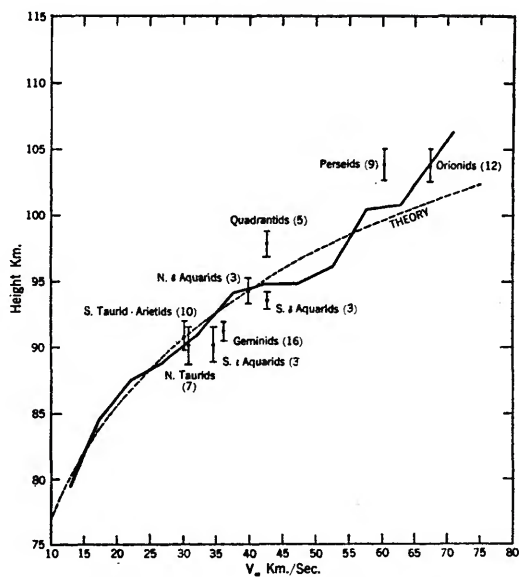


FIGURE 3.—Heights of maximum light for shower and sporadic meteors.

and $\log_e \rho_0 = -5.128$. The constant K_1 cannot easily be evaluated in terms of the variables in equation (19), and so K_1 was adjusted numerically until the theoretical curve gave the best fit with the observations. The theoretical curve shown in figure 2 is obtained by adopting $\log_e K_1 = -12.55$. There is obviously good general agreement between the theory and the observational data, although towards the high velocities, $V_\infty > 60$ km/sec, the observed heights are somewhat greater than we would expect. This may indicate a difference in composition of the group of sporadic meteors having these velocities.

In figure 3, the height of maximum light of shower meteors has been compared with the height for sporadic meteors. It can be seen that the showers differ noticeably: the Quadrantids and Perseids appear about 5 km higher, and the Geminids, southern δ Aquarids and southern δ Aquarids some 3 km lower, than the corresponding sporadic meteors. These differences in heights have been attributed by Jacchia (1956a, 1956b) to differences in composition of the meteoroids.

Relation between intensity and $\cos Z_{AR}$. If we substitute ρ_{max} from equation (14) and

m_{\max} from equation (16) into equation (12), we find that

$$\log_{10} I_{\max} = \log_{10} \left(\frac{2}{9} \frac{m_{\infty} v^3 \tau}{H} \right) + \log_{10} \cos Z_{AR}. \quad (22)$$

Substitution for I from equation (9) yields the expression

$$M + 2.5 \log_{10} m_{\infty} v^3 = K_2 - 2.5 \log_{10} \cos Z_{AR}, \quad (23)$$

where

$$K_2 = 22.9 - 2.5 \log_{10} \left(\frac{2\tau}{9H} \right), \quad (24)$$

and where τ , in equation (24), has the value assumed in computing m_{∞} .

Thus we may check the dependence of the intensity of maximum light on the zenith angle of the radiant by plotting the quantity $M + 2.5 \log_{10} m_{\infty} v^3$ against $\log_{10} (\cos Z_{AR})$. In figure 4 these values have been plotted for all meteors. For comparison a straight line has been drawn having the gradient predicted by the theoretical equation (23). The scatter of individual points is wide, but the general tendency is in fair agreement with the predictions of theory.

The theoretical light curve. A simplified form of the normalized light curve is given in equation (17). If we substitute for the isothermal atmosphere from equation (20), and for the relation between intensity and magnitude from equation (9), we find that

$$\begin{aligned} \frac{2.303}{2.5} (M_{\max} - M) &= \log_{10} \frac{9}{4} + \frac{h_{\max} - h}{H} \\ &+ 2 \log_{10} \left[1 - \frac{1}{3} \exp \left\{ \frac{h_{\max} - h}{H} \right\} \right]. \end{aligned} \quad (25)$$

In this analysis the magnitude of the meteor was measured at three points, the position of maximum light, and at the beginning and end of the trail when the magnitude of the meteor equalled the limiting magnitude of the plate, M_{lim} . Thus

At the beginning of the trail:

$$h = h_B, M_{lim} - M_{\max} = \Delta M.$$

At the end of the trail:

$$h = h_E, M_{lim} - M_{\max} = \Delta M.$$

It is therefore possible to check the theory by plotting ΔM against $h_{\max} - h_B$ and against $h_{\max} - h_E$. This has been done in figure 5 for

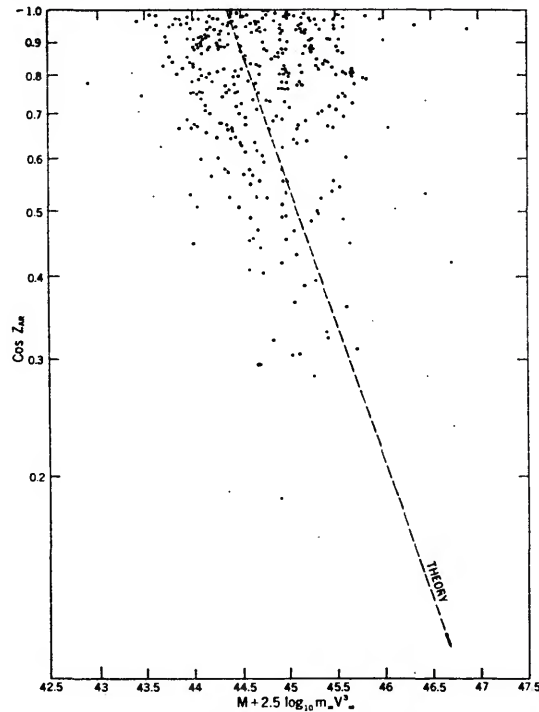


FIGURE 4.—Intensity of maximum light for all meteors, plotted against $\cos Z_{AR}$. Straight line indicates gradient predicted by theory.

the beginning and end of each of the meteors measured in the present program; the theoretical light curve as given by equation (25) is shown for comparison. Almost all of the meteor measurements are seen to lie within the theoretical light curve, illustrating the fact that the length of a meteor trail is considerably shorter than that predicted by the theory. Jacchia (1955) has suggested that this discrepancy can be accounted for by the phenomenon of fragmentation of the meteoroid. The results of any investigations, such as the study of meteors by radar, which have been based on the validity of the normalized curve must therefore be treated with the utmost reserve.

Acknowledgments

The photographic equipment used for this work was constructed and operated under contracts with the Air Force Cambridge Research Center and the Office of Naval Research. A few of the meteors included in the sample for statistical homogeneity have been previously re-

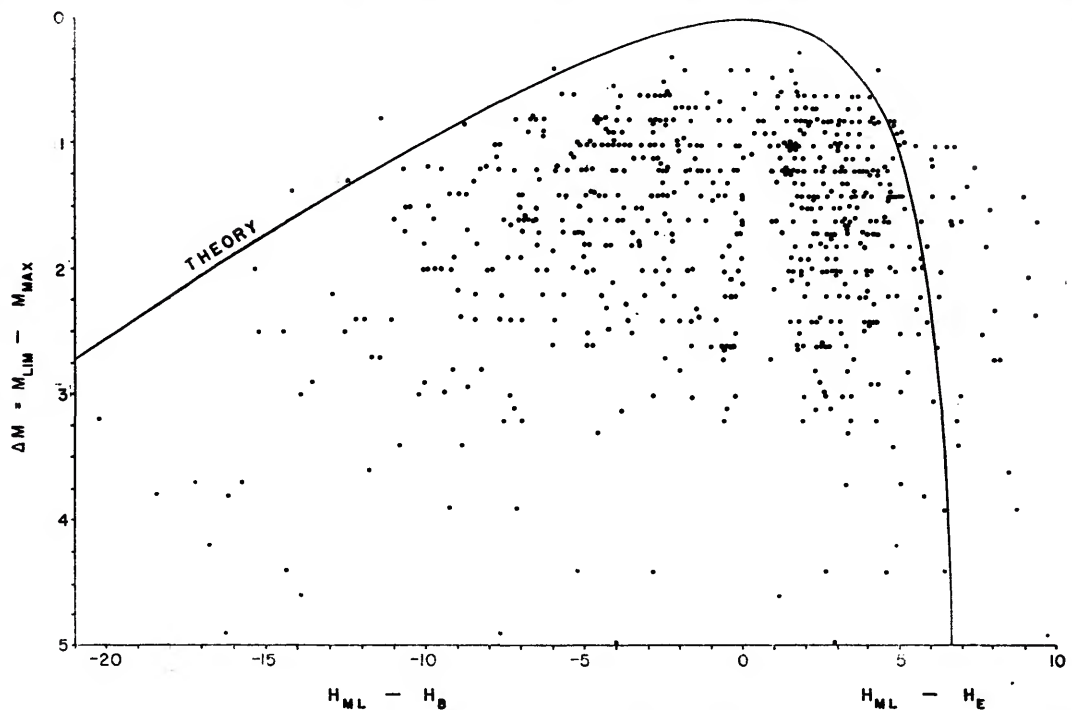


FIGURE 5.—Theoretical light curve compared with beginning and end points of observed light curves of meteors (see p. 354).
Key: H_{ML} , height at maximum light; H_B , height at beginning of observed trail; H_E , height at end of observed trail.

duced by Dr. L. G. Jacchia under contract with the Office of Ordnance Research. Dr. F. L. Whipple has directed the entire program of the Meteor Department at Harvard College Observatory and his advice on details and general planning of the Short Trail Reduction Program has been greatly appreciated. The assistance of Miss F. W. Wright has been invaluable in organizing the classification of photographic plates and the search for meteor trails. Much of the measurement and reduction has been carried out by Mrs. M. E. Greber, Mrs. D. Underhill, Mrs. V. Krotkov, Mr. R. F. Kandel, Mr. R. S. Calusdian, and Mr. P. Asch. Dr. R. E. McCrosky has assisted in supervising the work of the program. The measurements, reductions, and final preparation of the data were supported jointly by the Army, Navy, and Air Force, under contract with the Massachusetts Institute of Technology.

References

- HAWKINS, G. S.
1957. Smithsonian Contr. Astrophys., vol. 1, No. 2, p. 207.
- JACCHIA, L. G.
1955. Astrophys. Journ., vol. 121, p. 521.
1956a. Astron. Journ., vol. 61, p. 6.
1956b. Sky and Telescope, vol. 15 (March), p. 207.
- ÖPIK, E.
1937. Publ. Observ. Astron. Univ. Tartu, vol. 24, No. 5.
- ROCKET PANEL
1952. Phys. Rev., vol. 88, p. 1027.
- WHIPPLE, F. L.
1943. Rev. Mod. Phys., vol. 15, p. 246.
1954. Astron. Journ., vol. 59, p. 201.
- WHIPPLE, F. L., AND JACCHIA, L. G.
1957a. Astron. Journ., vol. 62, p. 37.
1957b. Smithsonian Contr. Astrophys., vol. 1, p. 183.
- WRIGHT, F. W., AND WHIPPLE, F. L.
1950. Harvard Repr., ser. 2, No. 35.

TABLE 1.—Fundamental data for sporadic meteors

Date (Universal time)	Height (km) at			Corrected radiant (Eq. 1950.0)		Cos Z_{AR}	Corrected velocity (V_∞)	Maximum photo- graphic magnitude (M_{pm})	Magnitude above plate limit (ΔM)
	Begin- ning (h_B)	Max- imum light (h_{max})	End (h_e)	R. A.	Decl.				
52 Feb 26. 40208	94.6	86.7	85.3	164°33'	+21°51'	.908	22.1±.7	+2.6	1.0
52 Mar 21. 36111	99.6	93.2	91.3	205 52	+58 48	.906	23.9±.2	+2.6	0.9
52 Mar 28. 22500	92.2	89.3	86.7	267 21	+70 46	.484	24.2±.4	+1.9	1.3
52 Mar 28. 45222	99.8	93.7	90.0	274 3	+22 36	.864	52.5±.3	+0.2	2.1
52 Apr 2. 38125	93.9	90.5	85.7	261 47	+58 5	.809	30.1±.7	+1.4	1.1
52 Apr 22. 29792	95.7	88.6	86.9	219 12	-11 0	.732	31.5±.9	+1.6	1.4
*52 Apr 23. 32587	105.4	94.8	89.6	266 5	+42 47	.811	40.8	+1.3	1.5
52 Apr 26. 28750	83.9	83.3	81.4	195 18	-17 38	.686	18.5±.3	+1.1	2.2
52 May 19. 21518	81.6	81.5	81.0	57 28	+27 12	.321	11.5±.2	+2.2	1.3
*52 May 21. 36274	100.8	95.6	93.3	256 19	-25 24	.550	36.0	+1.3	1.7
*52 May 22. 28093	85.7	83.0	77.0	219 36	-9 40	.779	17.3	+2.2	1.1
52 May 24. 35000	103.2	93.5	91.1	294 38	+50 35	.863	40.9±.3	+1.0	1.6
52 May 31. 38916	106.1	102.8	96.2	308 6	+18 52	.891	55.5±.3	+0.9	1.3
52 Jun 17. 36898	87.9	85.7	82.7	238 21	+60 20	.764	20.6±.2	+0.1	2.2
*52 Jun 21. 42265	113.4	102.6	95.7	5 42	+18 28	.677	68.8	-0.6	3.4
52 Jun 24. 20301	87.2	83.7	78.4	257 49	-10 25	.727	21.0±.1	+1.8	1.0
*52 Jun 25. 22215	101.3	87.4	86.2	278 5	-10 22	.632	30.4	-1.6	4.6
*52 Jul 24. 34757	112.8	97.1	93.8	10 28	+36 46	.755	65.3	-0.8	3.7
52 Jul 27. 22387	87.2	85.5	82.8	297 34	-2 17	.795	24.4±.2	+1.4	2.0
52 Jul 29. 41137	111.8	104.7	95.9	14 2	+45 27	.915	58.4±.3	-1.1	3.9
*52 Aug 4. 46209	92.3	92.1	87.1	262 9	+74 52	.488	28.2	+0.5	2.5
52 Aug 16. 32917	87.1	83.5	80.3	2 24	-14 12	.625	31.3±4.8	+0.5	2.4
*52 Aug 18. 25543	103.7	96.4	93.2	273 28	+65 37	.781	31.0	-0.3	3.0
52 Aug 18. 44646	108.8	100.9	97.9	20 57	+56 9	.917	57.5±.3	+0.7	2.0
52 Aug 21. 23344	86.0	85.4	81.2	340 24	-5 18	.718	17.4±.5	+2.0	2.0
52 Aug 22. 20000	83.2	83.1	81.5	354 43	+11 49	.675	14.5±.3	+1.5	2.0
52 Sep 12. 11222	88.6	85.7	83.7	292 40	+36 15	.990	19.4±.5	+2.5	0.8
*52 Sep 14. 23858	115.9	108.3	98.5	57 58	+51 49	.467	64.2	-2.5	4.9
*52 Sep 14. 37389	92.4	84.9	80.6	2 30	-15 41	.665	25.0	+0.3	3.2
52 Sep 16. 33723	103.4	94.5	90.4	10 13	+5 58	.899	36.9±.8	+0.5	2.2
52 Sep 16. 33958	79.8	77.4	75.4	327 11	-8 58	.694	13.9±.3	+3.0	0.8
52 Sep 17. 47711	111.9	101.3	98.4	41 41	+39 51	.957	60.6±1.0	+0.9	1.7
52 Sep 17. 47750	103.5	99.8	97.6	90 12	-15 9	.578	59.3±2.1	+1.3	1.0
52 Sep 19. 23462	94.7	87.1	82.9	341 26	-6 18	.810	20.0±.8	+2.0	1.7
52 Sep 20. 28438	101.1	96.8	88.7	351 45	-4 53	.817	23.0±.2	+0.9	2.3
52 Sep 20. 29047	89.7	87.7	84.7	14 1	-18 50	.638	22.5±.2	+2.3	1.0
52 Sep 20. 37133	110.5	105.6	103.9	71 44	+23 41	.755	70.1±.5	+1.0	1.0
52 Sep 25. 17361	89.2	85.7	82.4	326 20	+41 54	.983	19.4±.3	+1.4	1.7
52 Sep 25. 17571	108.4	104.0	99.9	39 7	+67 54	.568	51.7±.2	+0.8	1.4
52 Sep 25. 36001	96.5	89.9	86.5	355 15	+5 28	.798	23.8±.2	+2.5	0.8
52 Sep 25. 36419	109.1	103.8	103.4	72 7	+6 39	.669	65.7±.7	+1.1	1.1
52 Sep 25. 47579	110.6	107.4	104.4	115 10	-1 40	.569	61.5±.3	+1.7	0.6
52 Sep 26. 33935	108.3	104.3	101.8	61 4	+23 10	.799	65.4±.5	+1.8	0.8
52 Sep 26. 43333	104.6	96.9	96.0	3 13	+36 32	.762	37.3±.7	+1.7	1.0
52 Sep 27. 30972	94.6	92.0	88.8	349 47	+18 29	.936	20.0±.2	+2.7	1.2

*Previously reduced by Jaccchia.

TABLE 1.—Fundamental data for sporadic meteors—Continued

Date (Universal time)		Height (km) at			Corrected radiant (Eq. 1950.0)		Cos Z_{AR}	Corrected velocity (V_∞)	Maximum photo- graphic magnitude (M_{pm})	Magnitude above plate limit (ΔM)
Beginning (h_B)	Max- imum light (h_{max})	End (h_e)	R. A.	Decl.						
52 Sep 27.	43247	115. 5	110. 5	106. 0	96°13'	-2° 9'	.616	68.7±2.0	+0.9	1.2
52 Sep 28.	33541	96. 1	91. 9	87. 6	24 32	-3 52	.819	30.2±.4	+2.3	0.8
52 Sep 28.	33834	98. 3	96. 4	95. 0	82 3	+38 11	.665	67.0±.3	+1.6	0.4
52 Sep 28.	48414	96. 6	94. 1	88. 3	24 32	+27 33	.741	45.6±.4	+0.9	1.9
52 Oct 9.	19742	79. 3	78. 8	76. 9	278 36	+30 10	.782	12.7±.2	-0.2	3.2
52 Oct 9.	19792	99. 0	93. 1	91. 3	13 17	+8 40	.807	25.2±.2	+1.9	1.2
52 Oct 12.	33141	95. 5	93. 4	91. 0	181 53	+81 25	.442	43.5±.2	+1.7	0.8
52 Oct 13.	27778	101. 5	91. 4	87. 1	18 32	+18 5	.969	26.8±.3	+2.2	1.7
52 Oct 14.	26667	85. 0	85. 0	82. 8	38 7	+4 36	.845	15.6±.7	+3.3	0.7
52 Oct 14.	34938	90. 3	84. 2	81. 6	37 21	-14 51	.694	33.3±.2	+0.7	2.6
52 Oct 14.	35291	96. 9	92. 5	89. 1	4 6	+45 47	.865	24.2±.3	+2.3	1.0
52 Oct 16.	21458	92. 9	84. 4	82. 8	359 29	-7 40	.811	17.5±.4	+2.6	1.3
52 Oct 16.	33880	113. 4	108. 4	100. 6	103 56	+18 39	.525	72.0±.2	+0.1	1.8
52 Oct 17.	40034	113. 5	109. 6	105. 3	102 24	+26 20	.823	70.6±.4	+1.0	1.6
52 Oct 19.	38057	107. 0	103. 4	102. 8	228 22	+71 56	.283	39.0±.1	+2.0	0.8
52 Oct 19.	44228	76. 3	73. 1	69. 8	50 11	-7 24	.865	11.4±.2	+2.3	1.8
52 Oct 19.	44444	98. 0	93. 3	90. 0	59 35	+3 44	.833	32.8±.3	+1.4	2.6
52 Oct 19.	44602	94. 9	91. 8	86. 8	167 16	+76 0	.550	45.0±.2	+0.0	2.2
*52 Oct 21.	27695	117. 7	103. 3	101. 5	95 22	+5 56	.311	67.0	-0.5	2.5
52 Oct 21.	32905	95. 3	93. 3	89. 6	52 43	-9 34	.736	38.9±.4	+2.0	0.7
52 Oct 21.	32940	87. 7	86. 0	84. 7	22 37	-10 27	.753	18.1±.2	+2.1	1.2
*52 Oct 22.	26372	118. 9	109. 8	107. 1	104 15	+26 32	.306	70.6	+0.1	1.9
52 Oct 22.	33227	111. 1	104. 8	103. 0	104 49	+36 1	.645	68.4±.3	+1.4	0.8
52 Oct 23.	49206	109. 6	102. 9	98. 3	140 45	+4 21	.700	60.6±.5	+0.7	1.6
52 Oct 23.	49348	111. 8	93. 4	87. 5	110 59	+49 46	.949	64.1±.2	-1.0	3.8
*52 Oct 24.	27733	116. 7	102. 8	99. 4	99 29	+33 49	.498	67.8	-0.6	2.2
52 Oct 24.	35000	84. 3	82. 6	81. 0	21 23	+0 34	.778	20.7±.2	+1.9	1.2
52 Oct 24.	42292	89. 5	83. 9	81. 1	61 3	+34 54	.973	36.2±.5	+1.1	2.0
52 Oct 27.	36228	102. 9	94. 2	90. 3	102 32	+74 27	.689	50.3±.2	+1.0	1.4
52 Oct 27.	48226	108. 3	103. 4	97. 8	130 46	+60 0	.838	58.6±.3	-0.2	2.5
52 Nov 12.	19033	91. 0	81. 8	78. 6	342 10	+22 5	.903	15.6±.1	+2.4	1.4
52 Nov 12.	19349	89. 8	85. 8	83. 8	339 51	+22 26	.908	14.4±1.0	+2.3	0.7
52 Nov 12.	26391	89. 6	87. 5	84. 2	342 58	+21 52	.744	15.5±.4	+2.2	0.7
52 Nov 15.	41654	100. 2	90. 1	87. 8	63 14	-4 58	.673	32.5±.1	+1.4	1.4
52 Nov 18.	50424	97. 5	94. 6	89. 9	185 43	+45 15	.737	56.6±.2	+1.1	1.4
52 Nov 20.	33769	96. 6	92. 0	87. 2	102 43	+34 17	.913	53.2±.3	+2.1	0.8
52 Nov 21.	37387	109. 5	108. 8	105. 7	142 59	+4 20	.527	70.8±.9	+0.7	1.2
52 Dec 9.	26560	90. 0	86. 2	82. 9	52 1	+24 3	.975	18.3±.2	+1.6	1.6
52 Dec 9.	26872	80. 4	75. 7	74. 1	44 51	+6 1	.876	16.5±.1	+1.4	2.0
52 Dec 10.	22380	89. 7	84. 2	80. 7	52 49	+24 3	.992	16.0±.2	+2.5	1.4
52 Dec 11.	18502	99. 7	93. 4	92. 3	103 18	+49 22	.665	34.3±.2	+1.9	1.1
52 Dec 14.	25625	78. 8	78. 8	77. 7	353 53	+20 25	.750	11.4±.9	+1.8	1.6
52 Dec 14.	51304	117. 3	100. 6	95. 6	169 24	+13 36	.937	71.3±.3	-1.6	4.2
52 Dec 14.	51538	103. 7	99. 6	97. 1	148 27	+31 53	.982	62.5±.5	+1.8	1.2
52 Dec 16.	50693	104. 3	101. 1	97. 6	139 33	-8 3	.710	58.9±.4	+1.9	1.1

*Previously reduced by Jacechia.

TABLE 1.—*Fundamental data for sporadic meteors—Continued*

Date (Universal time)	Height (km) at			Corrected radiant (Eq. 1950.0)		Cos Z_{AR}	Corrected velocity (V_∞)	Maximum photo- graphic magnitude (M_{ph})	Magnitude above plate limit (ΔM)
	Begin- ning (h_s)	Max- imum light (h_{max})	End (h_e)	R. A.	Decl.				
52 Dec 20. 44578	89.3	89.1	83.5	100° 0'	+27°10'	.819	29.3±.2	+0.8	2.1
53 Jan 13. 29493	98.2	96.6	94.9	118 23	+22 7	.979	25.6±1.2	+3.2	0.7
53 Jan 13. 45089	94.6	82.5	79.6	122 57	+41 48	.825	27.0±.1	+1.3	2.4
53 Jan 13. 45411	91.0	85.8	79.3	122 22	+33 11	.801	27.6±.9	-1.6	4.4
53 Jan 14. 22500	85.8	82.5	77.7	125 29	+38 58	.868	21.4±.2	+1.7	1.6
53 Jan 14. 34632	108.4	98.3	94.7	140 44	+5 34	.882	47.8±.2	+1.0	2.0
53 Jan 15. 21244	92.8	81.4	76.2	65 17	+19 18	.955	16.0±.6	+3.0	0.8
53 Jan 15. 40959	98.0	97.2	94.1	111 36	+34 37	.840	22.3±.2	+2.5	0.8
53 Jan 16. 40208	110.3	106.8	105.1	154 58	-26 3	.530	57.1±1.1	+0.6	1.8
53 Jan 16. 40235	103.2	98.5	91.8	152 40	+33 25	1.000	42.1±.5	+1.7	1.0
53 Jan 17. 20082	89.1	86.6	83.1	301 26	+83 44	.533	21.8±.2	+0.6	2.7
53 Jan 19. 19278	97.2	95.8	91.5	105 32	+31 53	.939	20.1±.2	+2.4	1.2
53 Jan 19. 42292	111.7	106.8	102.0	189 8	+17 12	.887	65.8±.6	+0.6	1.8
53 Jan 19. 42292	104.0	93.0	88.9	156 0	+40 44	.986	34.4±.4	+2.0	1.6
53 Jan 21. 37852	96.1	91.4	89.4	105 55	+24 52	.822	20.0±.2	+2.7	0.8
53 Jan 21. 47209	82.0	81.3	79.7	121 38	+85 42	.732	13.4±.3	+2.5	1.0
53 Jan 21. 47354	93.5	91.1	88.0	148 35	+6 34	.756	41.4±.4	+0.8	2.0
*53 Jan 23. 38956	95.8	86.3	84.4	117 52	+14 0	.810	22.7	+1.7	2.0
53 Jan 24. 44375	87.8	86.4	84.6	121 6	-20 11	.432	16.9±.1	+2.1	1.4
*53 Feb 5. 14883	102.2	93.4	88.6	147 15	+12 27	.486	31.7	-0.1	3.4
*53 Feb 10. 27808	104.9	74.4	68.8	142 14	+38 51	.985	27.4	-2.9	5.6
53 Feb 12. 38367	91.6	87.5	84.2	167 34	+24 44	.989	29.8±.4	+1.3	2.1
53 Feb 12. 50846	101.6	87.7	85.7	219 22	+19 49	.976	61.0±.3	-0.3	3.0
53 Feb 17. 20441	98.0	92.0	89.5	147 0	+9 42	.799	25.0±.5	+1.2	1.8
53 Feb 17. 20626	89.5	89.2	82.9	162 54	+26 12	.753	26.6±.2	-0.0	2.6
53 Feb 18. 35000	96.5	86.6	84.7	154 38	+17 43	.956	24.1±.3	+1.8	1.5
53 Feb 20. 37820	82.0	81.7	80.4	156 37	+1 7	.855	14.2±.3	+2.0	1.2
53 Feb 20. 41300	96.7	93.3	90.8	185 3	+3 59	.880	34.9±.3	+1.4	1.5
*53 Feb 21. 46448	108.0	94.5	90.4	254 53	+8 53	.690	64.4	-0.6	2.9
53 Mar 12. 17613	94.6	92.0	90.3	150 27	-15 9	.685	17.1±.7	+1.8	1.0
53 Mar 12. 27841	92.1	89.0	85.6	153 12	+12 11	.942	18.7±.2	+2.5	0.6
53 Mar 13. 29792	83.5	83.5	82.6	143 0	-6 34	.748	14.6±.3	+1.6	1.6
53 Mar 13. 29824	83.3	82.7	80.2	130 20	+47 37	.883	15.4±.3	+0.6	2.6
53 Mar 13. 37773	93.2	90.6	84.6	218 16	+24 19	.950	41.0±.3	+1.6	1.4
53 Mar 14. 16204	74.4	72.0	70.3	80 37	+0 15	.791	12.9±.3	+2.6	0.6
53 Mar 14. 34103	83.4	81.7	78.9	167 39	-3 6	.802	20.6±.2	+3.1	0.3
53 Mar 14. 44147	77.7	77.3	74.3	204 30	+14 26	.961	11.9±.2	+1.9	1.8
53 Mar 14. 44426	106.5	100.7	96.0	270 37	+30 56	.783	48.8±.4	+0.9	1.4
53 Mar 14. 44737	109.2	105.2	101.4	235 52	-10 41	.720	64.2±.7	+1.3	1.2
53 Mar 18. 33889	83.8	81.8	78.5	161 50	+31 47	.943	15.6±.2	+0.1	2.8
53 Mar 18. 33892	85.4	85.4	83.6	174 44	-2 48	.828	18.6±.4	+1.2	1.9
53 Mar 18. 44619	109.6	107.1	105.2	287 52	+0 59	.446	65.8±.5	+1.0	1.2
*53 Mar 19. 31853	86.6	81.0	78.6	174 46	+26 20	.988	21.6	+1.9	1.7
*53 Mar 19. 39518	99.8	87.4	82.7	172 12	+20 1	.821	24.7	+2.1	1.3
53 Mar 20. 42303	87.9	87.8	86.1	159 17	-9 1	.412	19.0±.3	+2.2	1.0

*Previously reduced by Jacchia.

TABLE 1.—*Fundamental data for sporadic meteors—Continued*

Date (Universal time)	Height (km) at			Corrected radiant (Eq. 1950.0)		Cos Z_{AR}	Corrected velocity (V_∞)	Maximum photo- graphic magnitude (M_{pm})	Magnitude above plate limit (ΔM)
	Begin- ning (h_B)	Max- imum light (h_{max})	End (h_e)	R. A.	Decl.				
53 Mar 21. 40029	94. 5	90. 1	84. 0	183°43'	+13° 0'	.839	26.0±.2	+2.1	1.0
53 Mar 21. 40331	88. 4	82. 4	78. 2	169 5	+14 13	.739	20.2±.2	+2.5	0.4
*53 Apr 4. 17230	86. 4	80. 8	76. 8	175 48	+57 23	.878	18.0	+1.8	2.2
*53 Apr 7. 28372	103. 9	93. 7	86. 7	218 22	+7 54	.819	32.7	+0.0	3.0
53 Apr 7. 35030	93. 6	91. 1	89. 4	203 28	-10 52	.732	30.2±.3	+2.1	0.5
53 Apr 9. 29081	89. 8	87. 2	86. 6	184 45	+20 55	.976	19.0±.4	+2.4	0.8
53 Apr 9. 35927	93. 8	88. 5	84. 5	209 51	+27 38	.989	22.4±.2	+3.0	0.6
53 Apr 10. 24583	83. 6	82. 3	79. 3	185 24	+53 42	.951	14.6±.7	+3.1	1.2
53 Apr 11. 14238	76. 0	75. 5	73. 4	108 1	+15 54	.932	10.6±.3	+2.8	1.4
53 Apr 11. 22535	93. 7	85. 7	79. 9	186 20	+8 57	.909	19.6±.8	+2.0	2.0
*53 Apr 11. 34984	86. 6	83. 8	79. 2	194 52	+1 24	.819	21.9	-0.6	4.4
53 Apr 13. 25625	96. 2	91. 9	87. 1	212 58	+33 27	.928	25.9±.3	+1.8	0.9
53 Apr 13. 25916	99. 1	96. 3	94. 9	224 22	-15 34	.525	37.0±.9	+1.8	0.8
53 Apr 13. 46416	109. 9	102. 2	98. 2	282 5	-7 8	.720	66.7±1.6	+0.7	1.1
53 Apr 14. 28612	84. 9	83. 8	82. 5	190 57	+1 23	.878	18.8±.3	+2.2	1.2
53 Apr 15. 24583	86. 5	84. 2	81. 5	178 55	-5 41	.822	18.8±.9	+2.1	1.2
53 Apr 15. 24742	78. 0	77. 2	74. 4	137 48	+14 1	.886	11.0±.3	+3.4	0.9
53 Apr 15. 35235	87. 5	87. 1	85. 3	92 51	+81 4	.557	18.0±.3	+2.2	0.8
53 Apr 15. 45282	104. 3	99. 2	95. 1	294 59	+38 4	.873	39.3±.3	+1.5	1.0
53 Apr 15. 45366	116. 1	104. 4	95. 8	314 8	-0 25	.492	67.3±.3	-1.8	3.6
53 Apr 15. 45669	108. 5	102. 0	98. 8	277 49	+8 29	.877	61.8±.5	+0.9	1.5
53 Apr 16. 28881	96. 3	89. 9	84. 5	210 27	+14 48	.946	23.4±.3	+2.9	1.0
53 Apr 16. 42532	87. 5	85. 7	83. 2	256 35	+59 48	.894	29.6±.3	+1.5	1.3
53 Apr 21. 36042	101. 9	97. 7	95. 8	263 21	+61 3	.827	32.4±.3	+1.8	0.9
53 Apr 21. 36280	85. 7	78. 6	75. 3	222 32	+42 40	.979	24.5±.2	+1.4	1.6
*53 Apr 21. 44645	100. 5	91. 6	88. 6	347 23	+25 20	.323	47.2	+0.1	1.9
*53 May 5. 28417	104. 5	96. 1	91. 4	239 7	-22 13	.546	36.8	+0.8	2.2
*53 May 6. 28495	90. 2	85. 1	81. 1	214 42	-14 51	.720	21.4	+1.4	1.7
53 May 7. 22324	93. 1	88. 6	85. 9	211 2	-10 35	.751	20.4±.2	+2.6	0.8
53 May 7. 33659	88. 9	88. 9	86. 6	249 42	+32 30	.987	24.1±.5	+2.1	1.4
53 May 7. 33958	85. 1	82. 5	78. 4	231 38	+40 25	.988	17.6±.2	+1.0	2.4
53 May 7. 33977	95. 2	94. 1	84. 7	250 4	-0 39	.830	40.2±.3	+1.1	1.6
53 May 8. 26605	82. 0	81. 3	78. 7	224 5	+7 15	.918	15.9±.8	+1.4	2.4
53 May 8. 38998	83. 3	82. 8	80. 1	231 47	+41 28	.943	16.2±1.2	+0.5	2.6
53 May 9. 35808	99. 1	94. 9	91. 0	222 40	+2 6	.806	23.7±.2	+1.0	1.8
53 May 9. 42072	81. 5	81. 0	78. 4	341 45	+63 52	.726	14.7±.3	+1.1	2.6
53 May 12. 26313	91. 4	89. 2	85. 9	246 40	-5 6	.712	25.2±.3	+1.1	1.7
53 May 12. 26667	96. 8	89. 1	86. 1	226 10	+20 2	.972	21.3±.6	+2.2	1.0
53 May 13. 16348	81. 3	81. 1	79. 6	178 2	+15 4	.971	13.6±.3	+2.5	1.2
53 May 18. 41332	83. 7	81. 9	77. 0	258 59	+28 59	.972	18.1±.31	+1.4	2.3
53 Jun 2. 22566	98. 0	91. 0	86. 8	255 40	+18 14	.865	23.9±.2	+1.0	1.9
*53 Jun 4. 20432	96. 9	92. 1	89. 1	262 22	-25 53	.360	30.8	+1.2	1.6
53 Jun 5. 17987	90. 3	87. 8	85. 3	161 1	+49 3	.842	14.8±.3	+2.1	1.1
53 Jun 6. 19792	91. 3	88. 8	87. 0	143 30	+57 53	.669	17.2±.5	+2.4	0.6
53 Jun 8. 28370	93. 7	91. 5	87. 4	293 45	+22 9	.784	47.2±.3	+1.2	1.7

*Previously reduced by Jacchia.

TABLE 1.—Fundamental data for sporadic meteors—Continued

Date (Universal time)		Height (km) at			Corrected radiant (Eq. 1950.0)		Cos Z_{AR}	Corrected velocity (V_∞)	Maximum photo- graphic magnitude (M_{pm})	Magnitude above plate limit (ΔM)
		Begin- ning (h_B)	Max- imum light (h_{max})	End (h_e)	R. A.	Decl.				
53 Jun	8. 28750	93. 9	89. 8	87. 0	255°30'	+37°53'	.995	25.0±.3	+1.7	1.0
53 Jun	8. 29039	96. 5	94. 6	91. 9	240 16	-9 27	.763	20.8±.3	+1.9	0.9
53 Jun	8. 37832	92. 6	90. 1	86. 7	266 16	-25 51	.513	32.4±.2	+1.3	1.3
53 Jun	9. 33150	102. 8	99. 3	96. 0	280 24	-22 20	.580	38.4±.3	+1.4	1.0
53 Jun	9. 33275	79. 9	79. 3	78. 3	196 43	+1 17	.564	12.8±.2	+0.6	2.7
53 Jun	13. 26806	92. 4	88. 6	79. 7	253 4	+46 50	.972	24.1±.2	+1.9	1.4
*53 Jun	13. 36281	111. 1	95. 8	90. 9	322 9	+10 56	.764	63.0	-0.4	2.0
53 Jun	16. 30529	95. 5	92. 8	90. 9	264 59	-28 36	.526	27.4±.3	+2.0	0.6
53 Jun	16. 31098	89. 7	88. 0	86. 9	269 44	-28 24	.524	29.0±.2	+1.6	1.0
53 Jun	20. 35000	87. 0	86. 8	84. 0	258 35	+50 23	.906	21.2±.4	+1.6	1.7
53 Jun	20. 43325	88. 7	88. 3	88. 1	261 40	-47 31	.166	16.5±.3	+2.2	0.4
53 Jul	10. 31681	95. 8	92. 6	90. 7	287 45	+60 52	.888	26.3±.3	+1.3	1.7
53 Jul	10. 40023	109. 1	104. 4	101. 2	23 8	+27 8	.646	67.6±.6	+0.4	1.2
53 Jul	15. 23777	88. 2	88. 2	86. 3	25 56	+62 36	.453	17.8±.2	+2.1	1.1
53 Jul	15. 28729	83. 7	81. 7	79. 4	263 20	+50 47	.927	16.0±.3	+0.9	2.4
53 Jul	15. 42229	95. 1	90. 2	88. 5	337 52	+18 2	.969	54.8±.4	+0.1	2.6
53 Jul	16. 40248	105. 8	103. 0	100. 8	11 44	+22 17	.805	67.1±.7	+1.6	0.6
53 Jul	24. 43319	110. 1	107. 3	103. 1	352 37	+42 32	.984	57.3±.6	+1.0	1.7
53 Aug	4. 22721	111. 6	107. 2	102. 7	5 43	+34 52	.454	63.3±.3	+0.4	1.6
*53 Aug	5. 35035	90. 6	89. 1	83. 5	343 40	-16 28	.675	25.5	+1.0	2.3
*53 Aug	5. 43212	100. 8	93. 8	85. 9	59 33	+83 10	.601	43.6	+1.3	1.5
53 Aug	6. 16985	83. 0	82. 8	79. 3	272 19	-27 21	.637	15.5±.2	+0.3	3.0
53 Aug	6. 17192	94. 8	94. 0	91. 6	331 55	-13 5	.304	30.9±.4	+1.4	1.1
53 Aug	6. 30833	93. 4	91. 2	86. 9	341 4	+45 42	.929	47.1±2.2	+2.1	0.8
*53 Aug	7. 39845	83. 4	82. 9	80. 6	253 58	+11 34	.330	13.7	+0.5	3.1
53 Aug	9. 23255	91. 6	89. 3	85. 8	257 5	+38 46	.898	17.4±.2	+1.7	1.6
*53 Aug	10. 22697	80. 7	71. 6	69. 3	266 52	-6 35	.794	14.5	+1.0	2.8
53 Aug	13. 35836	82. 5	82. 2	81. 2	302 27	-23 44	.600	13.6±.3	+1.3	2.1
53 Aug	13. 36031	108. 7	105. 9	104. 7	40 8	+36 41	.701	68.6±.6	+0.3	1.1
*53 Aug	13. 42525	84. 2	80. 2	77. 4	280 8	+26 33	.421	17.7	-1.5	5.0
53 Aug	13. 45457	109. 7	104. 6	103. 0	45 0	+12 49	.854	72.1±.6	+0.9	1.0
53 Aug	13. 45561	97. 8	96. 5	84. 5	341 16	+30 17	.857	47.8±.3	-0.0	2.4
53 Aug	13. 45625	95. 5	91. 7	89. 1	59 8	+65 58	.756	54.6±.4	+2.3	0.6
53 Aug	14. 44728	108. 0	101. 6	97. 9	37 7	+5 20	.838	68.7±.8	+0.1	2.2
53 Aug	14. 45417	109. 2	92. 0	87. 1	2 56	+43 38	.959	56.8±.7	-1.0	2.2
53 Aug	15. 42275	88. 0	87. 3	86. 9	270 12	+38 51	.410	16.9±1.2	+2.6	0.6
53 Aug	22. 41119	100. 2	92. 6	88. 9	343 7	+10 48	.846	29.6±.2	+1.9	1.2
53 Oct	2. 20670	93. 3	92. 8	88. 4	20 21	-15 59	.491	28.5±.3	+1.4	1.3
53 Oct	2. 31090	99. 0	89. 8	83. 5	5 21	+7 43	.907	24.8±.2	+1.3	2.0
53 Oct	3. 25367	83. 7	81. 4	79. 7	345 1	+28 31	.991	16.5±.3	+1.3	2.1
53 Oct	3. 29383	83. 0	82. 8	80. 0	343 7	+10 23	.886	15.7±.3	+1.2	2.2
53 Oct	3. 44375	106. 1	100. 8	95. 3	79 21	+38 29	.972	68.1±1.0	+0.8	2.0
53 Oct	6. 28447	91. 1	90. 2	86. 5	16 54	+1 58	.870	24.1±.3	+1.6	1.4
*53 Oct	7. 39307	87. 5	78. 9	76. 4	9 18	+0 18	.699	20.6	+0.6	2.9
53 Oct	9. 24410	87. 7	86. 2	81. 5	24 42	+15 34	.878	28.8±.3	+0.9	2.0

*Previously reduced by Jacch a.

TABLE 1.—Fundamental data for sporadic meteors—Continued

Date (Universal time)		Height (km) at Beginning Maximum End (h_B) light (h_{max})			Corrected radiant (Eq. 1950.0)		Cos Z_{AR}	Corrected velocity (V_∞)	Maximum photo- graphic magnitude (M_{pm})	Magnitude above plate limit (ΔM)
		R. A.	Decl.							
*53 Oct 31. 31647	9. 31647	112. 4	103. 8	102. 5	123° 8'	+66° 42'	.454	58. 0	+0. 6	1. 7
53 Oct 10. 21343	105. 1	93. 4	85. 2	36 0	+16 36	.708	37. 4±. 1	-0. 3	2. 7	
53 Oct 10. 31215	95. 0	93. 2	91. 0	12 16	-9 33	.766	21. 2±. 4	+2. 4	0. 7	
53 Oct 12. 33162	108. 5	101. 7	96. 8	52 33	+45 5	.941	52. 9±. 3	+1. 3	0. 9	
53 Oct 16. 42579	110. 9	104. 5	100. 8	98 36	+26 48	.909	70. 5±. 5	+0. 6	1. 6	
53 Oct 31. 24399	79. 1	78. 7	76. 8	29 25	+18 48	.970	14. 8±. 4	+1. 0	2. 6	
53 Nov 2. 35675	105. 7	104. 6	103. 5	97 39	+83 34	.624	43. 0±. 3	+1. 3	0. 7	
53 Nov 2. 36021	102. 3	92. 5	87. 9	57 45	+16 3	.958	35. 0±. 3	+1. 7	1. 2	
53 Nov 6. 33041	82. 8	81. 2	78. 6	15 50	-15 29	.593	16. 8±. 1	-0. 0	3. 0	
53 Nov 9. 27016	100. 0	98. 6	93. 1	84 34	-19 59	.387	41. 4±1. 0	+1. 2	1. 0	
53 Nov 11. 44044	92. 3	85. 1	82. 3	71 19	+48 45	.889	44. 1±. 3	-0. 6	3. 1	
53 Nov 13. 24583	83. 4	81. 7	80. 1	29 29	+0 35	.884	16. 6±1. 4	+0. 5	2. 4	
53 Nov 13. 41988	109. 1	99. 8	94. 8	104 1	+8 5	.904	61. 6±. 6	-0. 8	3. 0	
53 Nov 16. 41339	94. 9	90. 7	86. 8	80 1	+30 29	.971	39. 1±. 3	+0. 1	2. 5	
53 Dec 4. 35998	98. 9	93. 3	86. 6	77 19	+18 52	.940	29. 0±. 4	+0. 6	1. 6	
53 Dec 4. 43333	99. 5	91. 4	85. 4	69 38	-6 2	.508	26. 5±. 3	+1. 3	1. 2	
53 Dec 8. 31711	91. 2	87. 4	83. 7	74 31	+15 13	.952	24. 3±. 6	+1. 5	1. 2	
53 Dec 9. 40208	102. 9	90. 2	83. 3	126 33	+2 34	.853	58. 2±1. 0	-0. 4	1. 7	
53 Dec 10. 51604	105. 2	98. 3	94. 4	101 36	+7 40	.555	43. 9±. 3	+1. 0	1. 7	
53 Dec 11. 32126	82. 0	80. 3	78. 7	81 23	+14 26	.965	14. 4±. 3	+1. 5	1. 6	
53 Dec 12. 29396	86. 6	84. 5	79. 8	94 28	+28 40	.972	36. 4±. 3	+0. 4	1. 4	
53 Dec 12. 40883	96. 2	95. 4	90. 7	206 51	+58 12	.503	44. 7±. 2	+0. 3	1. 4	
53 Dec 13. 50766	106. 3	99. 3	97. 5	128 24	-9 31	.644	58. 2±. 4	+0. 9	1. 5	
53 Dec 15. 49848	106. 2	102. 0	98. 6	198 6	+24 17	.795	64. 8±. 5	+0. 9	0. 9	
53 Dec 27. 20060	91. 7	84. 5	80. 6	100 24	+9 17	.743	27. 5±. 2	+0. 9	1. 2	
53 Dec 30. 36336	84. 4	81. 5	78. 4	113 16	+25 19	.985	30. 7±. 6	+1. 6	1. 0	
53 Dec 31. 33958	82. 9	80. 6	77. 1	109 26	+57 21	.926	17. 7±. 4	+1. 1	1. 5	
*54 Jan 1. 44056	96. 5	85. 1	75. 7	19 49	+68 57	.423	18. 9	+0. 5	2. 7	
54 Jan 3. 44375	108. 7	104. 2	99. 2	175 55	+24 23	.940	64. 6±. 5	+0. 7	1. 4	
54 Jan 4. 49735	112. 0	102. 0	99. 1	202 58	+7 21	.812	71. 4±. 6	-0. 3	2. 0	
54 Jan 5. 39088	110. 1	109. 2	107. 3	197 39	-23 23	.190	68. 9±. 6	+0. 4	1. 3	
54 Jan 6. 26510	93. 8	91. 2	87. 6	105 58	-20 32	.607	32. 4±. 2	+1. 4	1. 4	
54 Jan 13. 51791	83. 9	82. 8	80. 2	207 14	+44 59	.962	17. 3±. 3	+0. 4	2. 6	
54 Jan 28. 17159	84. 6	84. 6	82. 2	114 25	+37 48	.899	21. 0±. 6	+0. 7	1. 4	
54 Feb 2. 48125	77. 9	77. 7	76. 0	165 48	+55 1	.910	12. 8±. 3	+2. 1	1. 5	
54 Feb 3. 35977	105. 8	99. 0	92. 3	175 47	+33 35	.956	44. 7±. 3	+0. 3	1. 6	
54 Feb 4. 51289	106. 5	102. 2	96. 3	240 7	+39 12	.915	51. 0±. 7	+0. 1	1. 8	
54 Feb 6. 38914	93. 2	76. 1	71. 0	152 3	+30 29	.973	29. 0±. 1	-1. 3	3. 7	
54 Feb 6. 42292	91. 8	87. 8	82. 6	145 24	+16 49	.830	28. 1±. 8	+3. 0	1. 0	
54 Feb 8. 42292	92. 3	86. 7	81. 1	251 35	+59 32	.642	32. 1±. 7	+0. 2	2. 0	
54 Feb 10. 40343	91. 1	90. 8	81. 4	171 7	+37 27	.993	34. 9±. 3	+0. 5	2. 1	
54 Feb 11. 42659	81. 6	81. 0	79. 3	106 24	+36 31	.629	13. 9±. 2	+1. 1	1. 9	
54 Feb 26. 30579	87. 0	84. 9	83. 5	153 14	+3 10	.885	22. 3±. 5	+2. 4	1. 0	
54 Mar 1. 36968	93. 0	81. 9	79. 7	159 17	+23 29	.931	20. 7±. 2	+0. 2	2. 5	
54 Mar 5. 29565	84. 3	78. 2	74. 1	113 33	+12 36	.805	13. 2±. 1	+1. 7	2. 0	

*Previously reduced by Jacchia.

TABLE 1.—*Fundamental data for sporadic meteors—Continued*

Date (Universal time)	Height (km) at			Corrected radiant (Eq. 1950.0)		Cos Z_{AR}	Corrected velocity (V_∞)	Maximum photo- graphic magnitude (M_{pm})	Magnitude above plate limit (ΔM)
	Begin- ning (h_B)	Max- imum light (h_{max})	End (h_e)	R. A.	Decl.				
54 Mar 5. 44662	87.7	83.0	80.2	179° 6'	+39°45'	.877	26.4±.2	+0.9	1.4
54 Apr 24. 15182	100.9	92.0	82.3	220 43	-20 12	.240	32.4±.2	-0.3	2.4
54 Apr 28. 30873	86.9	86.8	85.3	313 46	+68 20	.599	16.6±.2	+2.0	1.0
54 Apr 29. 13439	85.6	81.5	79.1	117 58	+28 50	.846	<30	+0.9†	1.2
54 Jun 3. 25929	78.8	76.9	76.6	76 55	+62 47	.539	12.2±.5	+1.6	0.9
54 Jun 4. 24583	83.9	83.9	81.8	244 59	+50 32	.950	18.2±.3	+0.8	2.1
54 Jun 4. 35000	94.8	93.4	86.9	271 9	-28 51	.501	38.4±.7	+1.1	1.0
*54 Jun 5. 26538	98.2	89.0	82.5	105 11	+58 35	.284	19.3	-0.5	3.9
54 Jun 8. 32663	91.7	88.1	83.8	288 22	-19 25	.577	39.6±.4	-0.1	2.3
54 Jun 9. 37083	99.0	95.2	92.2	267 41	+56 39	.905	26.7±.5	+1.9	0.9
54 Jun 11. 38442	89.4	84.9	80.1	255 54	+51 44	.871	24.4±.3	+2.4	0.8
54 Jun 23. 21042	94.0	91.1	88.7	267 49	+66 56	.804	25.9±.3	+2.4	0.8
54 Jun 24. 23159	99.6	98.6	97.4	286 22	-16 15	.508	36.6±.3	+1.4	0.6
54 Jun 25. 24461	83.8	81.0	78.3	237 49	+46 21	.959	18.8±.2	+0.7	3.0
54 Jun 29. 33144	83.6	81.9	80.2	300 18	+54 17	.936	17.0±.3	+0.2	2.6
54 Jul 3. 17241	87.4	87.3	84.4	277 28	+1 7	.670	25.2±.2	+0.4	1.7

†Assuming $V_\infty = 25$

*Previously reduced by Jacchia.

TABLE 2.—Fundamental data for shower meteors

Date (Universal time)		Height (km) at			Corrected radiant (Eq. 1950.0)		Cos Z _{AR}	Corrected velocity (V _∞)	Maximum photographic magnitude (M _{ph})	Magnitude above plate limit (ΔM)	Shower
		Beginning (h _B)	Maximum light (h _{max})	End (h _E)	R. A.	Decl.					
*52 Jun	29. 43208	98. 9	88. 4	86. 2	299°18'	-16° 4'	.602	32. 1	+1. 5	1. 5	S. tAquarid
*52 Jul	25. 44425	97. 3	93. 8	86. 1	335 53	-17 4	.613	43. 0	+0. 1	2. 5	S. δAquarid
52 Jul	27. 22705	99. 7	93. 0	89. 9	323 49	-6 49	.554	38. 5±. 2	+2. 0	0. 8	N. tAquarid
*52 Jul	28. 31172	96. 8	92. 3	88. 9	339 39	-16 28	.572	42. 7	-0. 7	3. 3	S. δAquarid
52 Jul	29. 40913	96. 1	94. 5	91. 7	340 10	-16 35	.662	42. 2±. 3	+1. 6	0. 8	S. δAquarid
52 Aug	22. 20417	98. 4	95. 6	91. 9	321 9	-2 9	.772	24. 3±. 6	+2. 2	1. 0	α Capricornid
52 Aug	25. 35970	100. 0	94. 0	89. 9	354 16	+4 42	.889	39. 0±. 2	+0. 6	2. 4	N. δAquarid
*52 Sep	17. 31692	97. 5	85. 6	83. 8	10 39	+1 24	.857	33. 8	+0. 8	2. 4	S. Taurid†
52 Sep	19. 37056	93. 9	91. 6	89. 9	16 48	+1 12	.862	26. 5±. 3	+2. 9	0. 3	S. Taurid†
52 Sep	20. 28367	98. 6	89. 2	86. 9	12 29	+2 13	.834	26. 9±. 2	+2. 1	1. 2	S. Taruid†
52 Sep	25. 36076	100. 4	93. 4	86. 4	22 51	+3 59	.885	31. 8±. 2	+2. 0	1. 6	S. Taurid†
52 Oct	13. 28086	101. 1	95. 4	91. 7	34 51	+9 12	.879	31. 4±. 4	+2. 7	0. 6	S. Taurid†
52 Oct	14. 35000	100. 2	94. 4	86. 9	41 24	+12 13	.938	31. 8±. 3	+1. 9	1. 2	S. Taurid†
52 Oct	16. 33975	105. 4	82. 8	79. 4	39 40	+17 26	.967	35. 7±. 1	+0. 5	3. 2	N. Taurid
52 Oct	19. 26487	96. 1	89. 1	84. 2	36 3	+10 7	.880	29. 2±. 1	+1. 8	1. 4	S. Taurid†
52 Oct	19. 38343	100. 8	91. 9	87. 0	38 51	+19 38	.936	28. 6±. 1	+1. 6	1. 4	N. Taurid
52 Oct	21. 37795	112. 7	107. 7	103. 1	95 12	+16 15	.803	67. 8±. 4	+1. 1	1. 2	Orionid
52 Oct	21. 43514	112. 5	100. 0	96. 8	95 30	+15 41	.926	67. 8±. 4	+0. 0	2. 5	Orionid
52 Oct	22. 40394	111. 6	101. 5	97. 6	95 9	+16 11	.880	67. 8±2. 6	-0. 3	2. 9	Orionid
*52 Oct	22. 47095	101. 4	86. 2	80. 1	33 37	+7 26	.535	27. 9	+0. 4	2. 5	S. Taurid
52 Oct	23. 32858	115. 7	92. 5	90. 4	96 43	+16 21	.633	68. 0±. 2	-1. 9	4. 5	Orionid
52 Oct	23. 37987	116. 1	107. 9	102. 6	95 14	+16 19	.825	69. 4±. 7	-0. 9	2. 8	Orionid
52 Oct	23. 38440	110. 5	103. 9	100. 6	96 48	+17 3	.829	68. 0±. 4	+0. 4	1. 6	Orionid
52 Oct	23. 45296	112. 4	108. 0	101. 6	96 41	+15 37	.947	68. 3±. 5	+0. 1	2. 2	Orionid
52 Oct	23. 45794	110. 7	103. 7	96. 9	94 50	+16 55	.960	66. 5±. 3	-0. 6	3. 2	Orionid
52 Oct	23. 49375	111. 4	104. 4	100. 2	96 3	+15 42	.953	67. 2±. 5	+0. 4	2. 4	Orionid
52 Oct	23. 49586	110. 6	104. 7	100. 9	97 1	+15 50	.954	68. 3±. 6	+0. 7	1. 6	Orionid
52 Oct	24. 42326	112. 1	103. 8	99. 7	95 24	+16 54	.927	66. 9±. 9	+1. 0	1. 2	Orionid
52 Oct	27. 35625	98. 1	94. 2	89. 3	52 30	+12 32	.942	33. 3±. 5	+2. 1	1. 0	S. Taurid
52 Oct	27. 35799	100. 8	93. 7	89. 0	42 34	+18 55	.951	31. 1±. 5	+2. 6	0. 8	N. Taurid
52 Nov	7. 10870	96. 8	87. 1	83. 0	22 55	+27 33	.806	20. 9±. 2	+1. 2	2. 0	Bielid
52 Nov	12. 19596	98. 9	89. 0	85. 8	58 22	+22 58	.782	30. 7±. 2	+0. 9	2. 0	N. Taurid
52 Nov	12. 37045	98. 8	87. 8	81. 9	57 7	+22 7	.941	29. 8±. 1	+0. 7	2. 4	N. Taurid
52 Nov	12. 37333	106. 8	93. 0	86. 7	63 3	+25 4	.973	32. 0±. 5	+2. 4	0. 9	N. Taurid
52 Dec.	11. 25625	97. 4	91. 9	91. 0	110 11	+33 5	.798	36. 3±. 3	+1. 3	1. 2	Geminid
52 Dec.	14. 15038	99. 4	92. 1	89. 8	113 25	+32 8	.394	36. 6±. 0	+0. 5	2. 4	Geminid
52 Dec.	14. 25344	100. 8	86. 4	83. 8	113 36	+32 17	.784	36. 2±. 1	-1. 2	4. 4	Geminid
52 Dec.	14. 25988	96. 0	90. 7	88. 4	112 43	+32 10	.811	37. 0±. 2	+1. 5	1. 7	Geminid
52 Dec.	14. 44600	99. 4	91. 7	87. 9	113 27	+32 18	.948	36. 1±. 1	+0. 8	2. 4	Geminid
52 Dec.	14. 51668	97. 6	94. 3	91. 4	113 13	+32 5	.771	36. 2±. 2	+0. 8	1. 5	Geminid

†The Arietid stream, included in this category, appears to be indistinguishable from the Southern Taurids (see Wright and Whipple, 1950).

*Previously reduced by Jacchia.

TABLE 2.—*Fundamental data for shower meteors—Continued*

Date (Universal time)		Height (km) at			Corrected radiant (Eq. 1950.0)		Cos Z _{AR}	Corrected velocity (V _∞)	Maximum photographic magnitude (M _{pm})	Magnitude above plate limit (ΔM)	Shower
		Beginning (h _B)	Maximum light (h _{mes})	End (h _E)	R. A.	Decl.					
52 Dec	14. 51848	97. 9	93. 0	90. 3	114°50'	+31°45'	.779	35. 8 ± 1. 3	+0. 9	1. 4	Geminid
53 Jul	21. 35918	92. 1	89. 3	86. 7	328 34	-13 54	.700	35. 9 ± .5	+0. 7	2. 0	S. & Aquarid
53 Aug	5. 24597	103. 2	96. 2	91. 6	36 8	+55 14	.359	61. 0 ± .2	+0. 3	1. 5	Perseid
*53 Aug	8. 19278	101. 3	92. 9	88. 8	335 7	-15 6	.343	36. 1	+0. 8	2. 4	S. & Aquarid
53 Aug	8. 35862	108. 6	102. 3	101. 3	42 19	+56 41	.659	60. 7 ± .4	+0. 9	0. 9	Perseid
53 Aug	8. 36042	94. 3	90. 2	86. 5	309 46	-6 20	.712	23. 5 ± .3	+2. 2	0. 9	α Capricornid.
53 Aug	8. 36458	108. 3	101. 8	98. 1	41 4	+57 9	.682	60. 6 ± .3	+0. 9	0. 8	Perseid
53 Aug	8. 40951	110. 5	108. 0	103. 9	43 48	+60 54	.753	58. 6 ± .4	+0. 5	1. 2	Perseid
53 Aug	10. 35729	107. 8	101. 4	98. 8	40 42	+58 56	.678	59. 8 ± .4	+0. 3	1. 7	Perseid
53 Aug	10. 43442	97. 4	93. 2	89. 9	342 48	+0 29	.779	40. 5 ± .3	+1. 7	1. 3	N. δ Aquarid
53 Aug	13. 19186	98. 1	95. 8	94. 7	342 59	+2 32	.470	40. 0 ± .4	+1. 8	0. 6	N. δ Aquarid
53 Aug	13. 36156	110. 4	107. 2	104. 1	48 13	+59 5	.658	59. 5 ± .4	+1. 0	1. 0	Perseid
53 Aug	14. 36275	109. 4	107. 1	100. 3	49 12	+55 58	.663	61. 5 ± .3	+0. 1	1. 4	Perseid
53 Aug	15. 41947	110. 3	106. 5	100. 3	52 36	+52 22	.791	63. 3 ± .5	-0. 0	3. 1	Perseid
53 Aug	15. 44366	106. 8	104. 3	100. 3	53 4	+57 28	.818	60. 2 ± .5	+1. 0	0. 8	Perseid
*53 Oct	9. 19222	103. 8	96. 3	90. 6	270 56	+47 14	.669	20. 2	+0. 1	1. 6	Giacobinid
53 Oct	9. 24725	99. 8	89. 7	87. 5	34 8	+7 44	.772	30. 4 ± .2	+1. 6	1. 8	S. Taurid
53 Oct	19. 42117	110. 7	106. 7	105. 6	93 17	+15 46	.903	65. 3 ± .8	+1. 6	0. 4	Orionid
53 Nov	3. 29681	101. 6	92. 9	88. 7	47 35	+21 17	.978	28. 8 ± .3	+2. 5	0. 8	N. Taurid
*53 Nov	7. 46139	86. 2	81. 2	79. 1	31 4	+12 40	.448	19. 8	+1. 7	1. 9	Bielid
53 Dec	12. 34620	97. 1	90. 6	89. 2	111 47	+32 47	.980	35. 7 ± .3	+1. 2	1. 2	Geminid
53 Dec	12. 49241	99. 6	91. 2	88. 5	111 27	+32 17	.848	35. 9 ± .3	+1. 3	1. 8	Geminid
53 Dec	13. 31502	100. 1	94. 8	91. 5	112 55	+32 39	.934	36. 0 ± .2	+1. 4	1. 1	Geminid
*53 Dec	13. 36370	98. 4	87. 0	79. 4	112 6	+32 39	.994	36. 3	-0. 2	2. 2	Geminid
53 Dec	13. 43578	100. 8	93. 2	87. 5	111 53	+32 49	.962	36. 5 ± 1. 0	+0. 2	2. 2	Geminid
53 Dec	13. 46534	95. 7	91. 9	89. 9	112 31	+32 24	.914	35. 6 ± .3	+1. 3	1. 5	Geminid
53 Dec	14. 37933	98. 8	94. 3	87. 0	112 52	+32 27	1.000	36. 4 ± .2	+1. 0	1. 4	Geminid
*53 Dec	14. 40912	100. 3	84. 1	70. 6	113 9	+32 20	.991	36. 2	-2. 5	4. 9	Geminid
53 Dec	14. 47656	97. 3	92. 2	88. 4	111 54	+31 5	.876	36. 4 ± .4	+1. 6	1. 5	Geminid
54 Jan	2. 37141	102. 0	98. 7	94. 8	226 13	+51 6	.365	42. 8 ± 2	-0. 0	1. 8	Quadrantid
54 Jan	3. 36061	100. 9	99. 4	97. 8	231 1	+50 29	.294	42. 1 ± .3	+0. 7	1. 1	Quadrantid
54 Jan	3. 36219	101. 0	99. 4	96. 9	230 4	+49 12	.295	42. 7 ± .2	+0. 9	1. 4	Quadrantid
54 Jan	3. 47494	100. 2	95. 3	93. 0	228 40	+50 26	.672	42. 2 ± .3	-0. 2	2. 0	Quadrantid
54 Jan	3. 50625	99. 6	96. 6	93. 4	229 29	+48 26	.755	43. 4 ± .5	+0. 6	1. 6	Quadrantid

*Previously reduced by Jacchia.

Abstract

A random sample of 360 of the meteors doubly photographed by the Baker Super-Schmidt cameras has been taken. These meteors are fainter than those previously reduced, reaching a limiting photographic magnitude of +4. Their heights, velocities, radiants, and magnitudes have been accurately computed and are tabulated. Current meteor theory is briefly outlined, and certain of its predictions compared with statistics of the observed sample of meteors. The observed length of trail is less than that predicted by the single-body theory.

